URSI GASS 2021, Rome, Italy, 28 August - 4 September 2021

Preliminary investigations on microwave hyperthermia for breast cancer using a dipole antenna.

Jeantide Said Camilleri* (1), Iman Farhat(1), Lourdes Farrugia(1), Julian Bonello(1) and Charles V. Sammut(1)
(1) Department of Physics, Faculty of Science, University of Malta, MSD 2080 Msida, Malta.

Abstract

This paper presents an investigation of two dipole antennas working at 434 MHz and 2.45 GHz as a tool to understand the mechanisms to optimise microwave hyperthermia (MWH) for breast cancer. The investigations were performed on a numerical breast phantom with a water bolus kept at 25 °C developed in CST Studio Suite. The bolus thickness and dipole placements with respect to the breast were varied and an optimal scenario was selected. A layer of fat was then added to these models where the effect of fat on the temperature distribution was investigated. The results show that the 434 MHz dipole requires further improvements, but a hotspot located well below the surface of the breast suggests its usefulness for deep-seated tumours. In contrast, the 2.45 GHz dipole is a good candidate for superficial MWH where the matching, power required and hotspot focusing were superior.

1 Introduction

The most frequently diagnosed cancer affecting females is breast cancer, making up 25% of the female global cancer cases [1]. The most common courses of action for breast cancer treatment are lumpectomy, partial or radical mastectomy, which require surgery to remove the tumour or the whole breast. Other forms of therapy such as radiotherapy or chemotherapy are also commonly used to treat breast cancer and can be applied before or after surgery [2].

Hyperthermia is a non-invasive therapy where a region of the body is heated to 42-45 °C for 60-90 minutes [3]. When applied to cancerous cells, the rise in temperature does not cause cell death, but it inhibits a repair mechanism within the cells when subjected to radio or chemotherapy. The temperature increase blocks the cells from repairing any damage caused by sublethal attacks, making the cells more sensitive to radiotherapy or chemotherapy [4]. It has been shown that hyperthermia increases the effectiveness of radiotherapy or chemotherapy when jointly administered in the treatment of breast cancer [5]. Microwave hyperthermia (MWH) is an emerging therapy which uses non-ionising radiation to increase the cell temperature. However, further investigation is required to localise heating and minimise damage to healthy tissue when using MWH.

This paper presents a preliminary investigation of two dipole antenna designs working at 434 MHz and 2.45 GHz for deep and superficial MWH, respectively. The antennas are easy to build and cost effective due to their simple components. The antennas were simulated in the CST Studio Suite (CST), where their effect on a breast phantom was examined, analysing variations due to the different antenna positioning with respect to the phantom, the water bolus thickness, increasing complexity of the tissue by adding fat and the input power.

The rest of the paper is divided as follows. The methodology of the investigation is presented in Section 2, followed by the results obtained in Section 3. A discussion on the results and future work is given in Section 4.

2 Methodology

Two dipoles were investigated for their usefulness for MWH for breast cancer, one working at 434 MHz and one at 2.45 GHz. The dipole geometries are described in Section 2.1. The dipoles were then tested on a breast phantom, modelled as described in Section 2.2 with varying water bolus thicknesses and placement of the dipole. Sections 2.3 and 2.4 describe the simulation settings. In Section 2.5, the complexity of the model was then increased by adding fat to investigate its effect on the antenna's heating capability.

2.1 Antenna Structure

The dipole antennas were designed in CST as shown in Figure 1. These antennas consisted of two coaxial cables whose inner conductors were connected to each other whilst the outer conductors were connected to the dipole arms. The dielectric of the coaxial cables was lossy PTFE whilst the rest of the dipole was constructed using perfect electrical conductor (PEC). The dimensions for each dipole are given in Table 1 and Table 2. Once the dipoles were optimised to work at the desired frequencies, they were then tested upon breast phantom models.

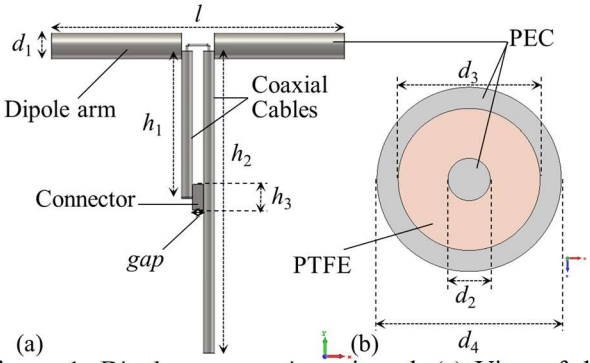

Figure 1: Dipole structure investigated. (a) View of the dipole, dimensions given in Table 1. (b) A cross-section of the coaxial cable, dimensions given in Table 2.

Table 1. Dimensions of dipole antennas working at 434 MHz and 2.45 GHz.

Frequency	L (mm)	h_1 (mm)	h_2 (mm)	h_3 (mm)	*gap* (mm)
434 MHz	335.38	172.70	345.38	5	2
2.45 GHz	56.00	30.59	61.18	5	2

Table 2. Values of the coaxial cable diameters for the two antennas working at 434 MHz and 2.45 GHz.

Frequency	d_1 (mm)	d_2 (mm)	d_3 (mm)	d_4 (mm)
434 MHz	6.00	1.00	3.40	3.90
2.45 GHz	5.10	0.50	1.68	2.18

2.2 Numerical Breast Phantom

The breast phantom consisted of a hemisphere of breast glandular tissue of diameter 140 mm and a 2 mm layer of skin added over the breast tissue. The chest wall consists of a 170×10×170 mm block of muscle fat and 170×5×170 mm of muscle as shown in Figure 2. In subsequent simulations, the phantom was altered to add a 2 mm or 5 mm layer of fat between the skin and the breast glandular tissue. A distilled water bolus kept at a constant temperature of 25 °C encased the hemisphere which not only cools the skin surface and minimises hotspots, but also improves the impedance matching of the antenna [6]. The dielectric and thermal properties of the tissues used (from the software's material library) are shown in Table 3.

2.3 Electromagnetic Simulations

A total of nine simulations per dipole were carried out to investigate the effect of the bolus thickness (BT) and the distance of the dipole from the bolus (DB). These were set to values of 5, 10 and 15 mm. The electromagnetic (EM) simulations gave information on the impedance matching of the antenna and the energy dissipated through the tissue. The boundary conditions for the simulations were set to open (add space) and the background was set to air. The transient solver employed a hexahedral mesh of 15 cells per wavelength for both the 434 MHz and 2.45 GHz dipole. The number of cells per wavelength was later reduced to seven cells per wavelength when adding fat to the model in the case of the 2.45 GHz dipole, to reduce computational time. The input power was set to 50 W for the 434 MHz dipole whilst the power was set to 5 W for the 2.45 GHz dipole.

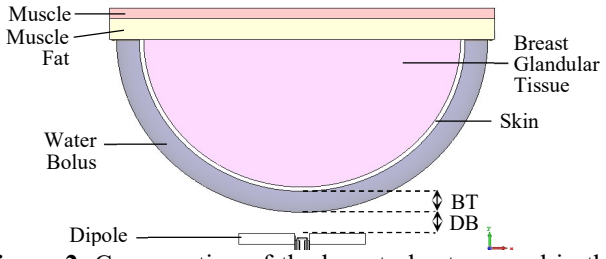

Figure 2. Cross-section of the breast phantom used in the investigations, where BT is the variable bolus thickness and DB is the variable distance between the dipole and the bolus.

2.4 Thermal Simulations

The thermal simulations were carried out using the EM-Thermal hybrid solver within CST, which uses the previously calculated EM simulation to calculate the temperature distribution within the tissue. For both dipoles, a hexahedral mesh of 20 cells per max model box edge was used. The boundaries were set to isothermal (at 25 °C) and the background as air. The simulation was set to run for an exposure time of 2 hours, to completely cover the duration of a hyperthermia procedure. The ambient temperature was set to 25 °C and the bioheat setting was activated with a blood temperature of 37 °C. The solver employed Pennes' bioheat equation to calculate the temperature distributions, using the thermal properties given in Table 3.

2.5 Increasing Model Complexity

After the nine simulations were carried out, the optimal values of BT and DB were determined through the impedance matching and temperature distributions obtained. The selected model was then further investigated by adding a 2 mm and a 5 mm layer of fat under the skin layer, subtracting these from the breast tissue to keep the overall hemispherical radius fixed, as shown in Figure 3. In these cases, the input power was also increased to obtain the desired temperature increase within the tissue.

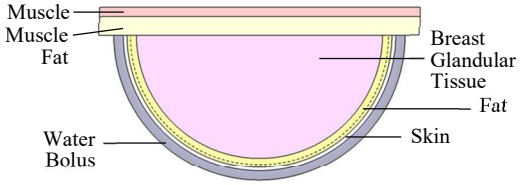

Figure 3. Cross-section of modified breast phantom with the dashed line showing an approximate 2 mm layer.

Table 3. Dielectric and thermal properties for the materials used for the breast phantom.

Materials	ε' at 434 MHz	ε'' at 434 MHz	ε' at 2.45 GHz	ε'' at 2.45 GHz	Thermal Conductivity (W K^{-1} m^{-1})	Specific Heat (J K^{-1} kg^{-1})	Density (kg m^{-3})	Bloodflow Coefficient (W K^{-1} m^{-3})	Basal Metabolic Rate (W m^{-3})
Distilled Water	78.400	0.000	78.400	0.000	0.600	4200	998	0	0
Skin	46.044	29.234	38.011	10.757	0.293	3500	1100	9100	1620
Fat	5.569	1.731	5.280	0.768	0.210	2500	910	1700	300
Breast Glandular	61.334	36.829	57.210	14.510	0.620	3600	1020	3600	640
Muscle Fat	5.568	1.743	5.262	0.781	0.400	3000	1000	2000	400
Muscle	56.876	33.452	52.733	12.837	0.530	3546	1041	2700	480

3 Results

The results for the initial bolus thickness and dipole distance simulations are given in Section 3.1. Section 3.2 gives the results of the more complex phantom simulations and a comparison of the heating pattern obtained at the two different frequencies is given in Section 3.3.

3.1 Investigating BT and DB

The initial investigation involved comparing the results obtained when varying the values BT and DB. Table 4 shows the S11 magnitude (dB) as obtained for the nine different configurations at 434 MHz and 2.45 GHz. From this table, the two highlighted entries indicate the configurations which resulted in the lowest S11 at each frequency, thus having the best impedance matching.

Table 4. S11 magnitude in dB at 434 MHz and 2.45 GHz for the initial nine simulations.

BT (mm)	S11 Magnitude (dB)					
	DB (mm) for 434 MHz			DB (mm) for 2.45 GHz		
	5	10	15	5	10	15
5	–5.964	–6.371	–6.801	–10.393	–22.546	–15.474
10	–6.092	–6.438	–6.799	–9.058	–21.091	–17.905
15	–5.980	–6.284	–6.648	–12.698	–28.544	–16.938

From Table 4, it can be seen that the best matched phantom for the 434 MHz dipole was that with a bolus thickness of 5 mm and a dipole placed 15 mm away from this bolus. For the 2.45 GHz dipole, a bolus thickness of 15 mm and the dipole placed 10 mm away from the bolus gave the best impedance matching. Figure 4 compares the S11 of these scenarios to the S11 obtained for each dipole without a phantom present.

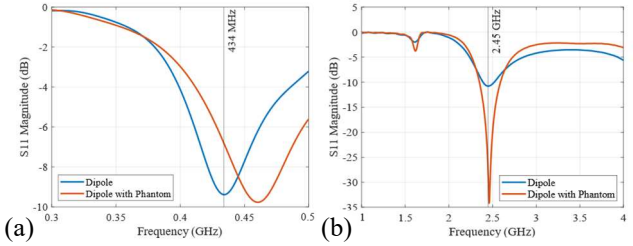

Figure 4. Comparison of the S11 obtained with or without a phantom present.

Following the EM analysis, the temperature distribution was also investigated. Figure 5 shows the cross-sections of the temperature profiles obtained after an exposure time of 2 hours for the two configurations identified in Table 4. These profiles were calculated from the EM simulations, ensuring that the time (2 hours) was sufficient to reach thermal equilibrium, as can be seen in Figure 6. Although the temperature might not have reached the desired range for these optimal impedance scenarios, adjusting the input power slightly proved enough to obtain the desired temperatures, as will be seen in the next section. Indeed, the maximum temperatures reached after 2 hours in this set of investigations were 44.50 °C for 434 MHz and 45.12 °C for 2.45 GHz.

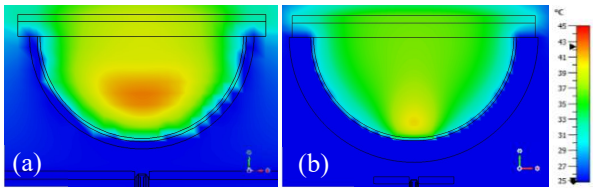

Figure 5. Temperature mapping of optimal BT and DB for (a) 434 MHz and (b) 2.45 GHz.

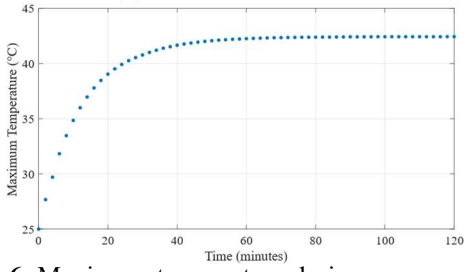

Figure 6. Maximum temperature during exposure for the identified 434 MHz phantom. All other simulations showed similar behaviour.

3.2 Adding Fat

In this section, the model configurations identified in Table 4 are further investigated by adding a 2 mm or 5 mm layer of fat as shown in Figure 3. This was done to investigate whether such an addition changed the hotspot nature. Figure 7 provides the normalised E-field through the phantom for varying fat layers. In addition, Table 5 gives the maximum temperature reached at each power setting variation for the fat layers, and the temperature mapping for the highlighted entries are shown in Figure 8.

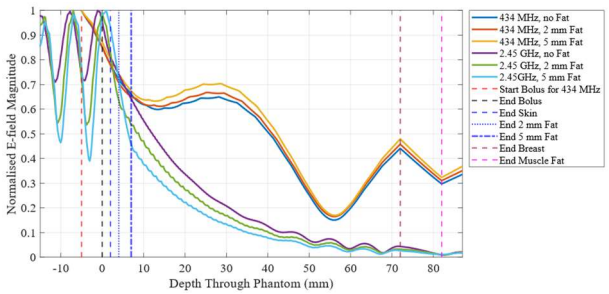

Figure 7. Normalised E-field through the centre of the phantom with varying layers of fat for both dipoles.

Table 5. Maximum temperatures reached after 2 hours of exposure for both dipoles.

Fat Thickness (mm)	Maximum Temperature (°C)					
	Power (W) for 434 MHz			Power (W) for 2.45 GHz		
	50	60	75	5.0	7.5	10.0
0	42.43	/	/	40.42	/	/
2	43.57	45.19	47.62	40.93	44.91	49.00
5	45.22	47.10	49.91	39.21	41.89	44.57

3.3 Comparing Frequencies

The two frequencies produced distinct hotspots and required different input powers to achieve the desired temperature increase. Figure 8 shows the highlighted simulations from Table 5 as a comparison of the thermal mapping of a phantom with the same fat layer (2 mm).

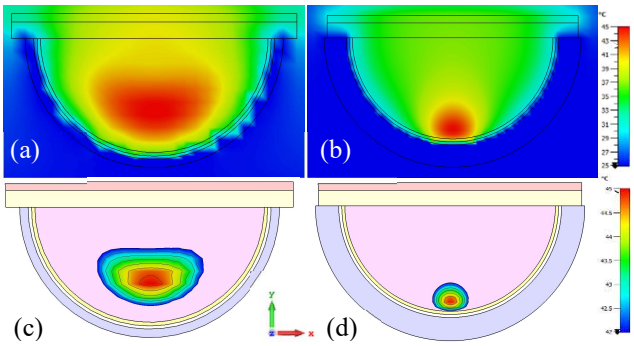

Figure 8. Thermal distributions for 434 MHz (a & c) and 2.45 GHz (b & d). The top images show the thermal distributions through the whole phantom while the bottom images show the hotspots (from 42 to 45 °C).

The hotspot generated at 434 MHz (Figure 8c) had a size of 63.0×34.2×46.7 mm, where the maximum temperature was reached directly above the dipole at a depth of 26.7 mm below the skin surface. In contrast, the hotspot generated at 2.45 GHz (Figure 8d) had a size of 23.3×18.1×23.2 mm, with a maximum temperature reached at 9.9 mm below the skin surface.

4 Discussion

This paper investigated two dipoles working at 434 MHz and 2.45 GHz as MWH applicators for breast cancer. The dipoles were first tested on a breast phantom, of mostly glandular tissue to mimic a dense breast, with a water bolus. The bolus thickness and the dipole placement were varied, and the impedance matchings obtained in each combination were compared.

Figure 4 presents the S11 plots obtained for both dipoles with the optimal combination of BT and DB. At 2.45 GHz, the impedance matching of the system improved significantly when comparing the dipole performance in free space to the dipole irradiating the breast phantom, but at 434 MHz, a mismatch was observed. It was also noted that the temperature range of 42-45 °C was only attainable at 434 MHz with a significantly larger input power of 50 W compared to the 5 W required when working at 2.45 GHz.

Next, a layer of fat was added to the breast phantom between the skin layer and glandular tissue. To compare the effect of fat, Figure 7 shows the normalised E-fields through the phantom with either 0, 2 or 5 mm of fat for both dipoles, where the power was kept at 50 W or 5 W for the 434 MHz and 2.45 GHz dipoles, respectively. At 434 MHz, the E-field magnitude increased with increasing fat. However, the opposite was observed when operating at 2.45 GHz. The longer wavelength of 434 MHz allowed for deeper penetration within the breast, so that a hotspot was formed deeper within the tissue. The deeper penetration at this frequency resulted in less absorption at the surface so that less energy was lost within the fat layer, therefore increasing the E-field magnitude within the glandular tissue.

The shorter wavelength of the 2.45 GHz dipole resulted in focussed microwave energy close to the surface, where a hotspot was formed. The energy was attenuated as the wave encountered the tissue. Since the energy was focussed at the surface of the model, increasing the fat layer resulted in more absorption at the surface, so that less energy reached the glandular tissue, as shown in Figure 7. Table 5 also shows these effects, where the maximum temperature reached within the tissue was increased with increasing fat for 434 MHz but decreased for 2.45 GHz.

Finally, the hotspots produced for both dipoles were compared in Figure 8. At 434 MHz, a much larger power was necessary to produce the required temperature increase than that used at 2.45 GHz. However, the maximum temperature was reached at a depth of 26.7 mm within the breast, suggesting this dipole could be useful for deeper located tumours. Future investigations with this dipole are required to obtain a better impedance matching when applied to the phantom. An array of such a dipole could also be investigated with the aim of reducing the hotspot volume and utilising less power. The hotspot obtained with the 2.45 GHz dipole reached a maximum temperature at 9.9 mm from the skin, with Figure 8 clearly showing the superficial MWH application. The optimal impedance matching obtained for this dipole, as shown in Figure 4, suggests that this dipole may be a good candidate for MWH for superficial breast cancers. Future work to investigate an array of 2.45 GHz dipoles to assist in localising the hotspot at the surface or at a particular location may also explore techniques to reduce the input power, thus making the MWH system more efficient.

References

[1] "GLOBOCAN 2020: New Global Cancer Data | UICC." https://www.uicc.org/news/globocan-2020-new-global-cancer-data.

[2] "Treatment and Side Effects." https://www.breastcancer.org/treatment.

[3] E. Zastrow, S. C. Hagness, and B. D. Van Veen, "3D computational study of non-invasive patient-specific microwave hyperthermia treatment of breast cancer," *Phys. Med. Biol.*, vol. 55, no. 13, pp. 3611–3629, Jul. 2010, doi: 10.1088/0031-9155/55/13/003.

[4] M. Mallory, E. Gogineni, G. C. Jones, L. Greer, and C. B. Simone, "Therapeutic hyperthermia: The old, the new, and the upcoming," *Crit. Rev. Oncol. Hematol.*, vol. 97, no. 2015, pp. 56–64, 2016, doi: 10.1016/j.critrevonc.2015.08.003.

[5] C. C. Vernon *et al.*, "Radiotherapy with or without hyperthermia in the treatment of superficial localized breast cancer: results from five randomized controlled trials," *Int. J. Radiat. Oncol. Biol. Phys*, vol. 35, no. 4, pp. 73–744, 1996.

[6] P. Togni, J. Vrba, and L. Vannucci, "Water bolus influence on temperature distribution of applicator for small melanoma tumors," *Eur. Microw. Week 2009, EuMW 2009 Sci. Prog. Qual. Radiofreq. Conf. Proc. - 39th Eur. Microw. Conf. EuMC 2009*, no. October, pp. 874–877, 2009, doi: 10.1109/EUMC.2009.5295957.